



Title	The Role of Sediment-Laden Underflows in Lake Sedimentation : Glacier-Fed Peyto Lake, Canada
Author(s)	CHIKITA, Kazuhisa
Citation	Journal of the Faculty of Science, Hokkaido University. Series 7, Geophysics, 9(2), 211-224
Issue Date	1992-02-29
Doc URL	http://hdl.handle.net/2115/8784
Type	bulletin (article)
File Information	9(2)_p211-224.pdf



[Instructions for use](#)

The Role of Sediment-Laden Underflows in Lake Sedimentation : Glacier-Fed Peyto Lake, Canada

Kazuhisa Chikita

*Department of Geophysics, Faculty of Science,
Hokkaido University, Sapporo 060, Japan*

(Received October 30, 1991)

Abstract

Dynamic effects of "sediment-laden underflows" on lake sedimentation are documented, using field data obtained in glacier-fed Peyto Lake, Canada during the glacier-melting period (June-August) of 1987. "Sediment-laden underflows" are here referred to bottom currents flowing continuously on an undulated bottom bed of lake with keeping relatively high suspended sediment concentration. The dynamic behavior of the sediment-laden underflows in Peyto Lake is outlined by some observational results of flow velocity, water temperature and sediment concentration. Sediment sorting processes of the sediment-laden underflows are specified by grain size distributions of the sediment trapped near the bottom. The fine sediment transported by the underflows probably sinks as non-flocculated, discrete grains within the bottom water of almost no salinity and low sediment concentration ($< \sim 80$ mg/l), because the sediment is almost dolomitic, thus including little cohesive clay mineral.

Sedimentation rates estimated for the underflows, the delta progradation and overflows and/or interflows account for 61%, 32% and 7% of the overall sedimentation, respectively, and offer the possible life span of 586 yrs.

1. Introduction

Sedimentation in glacier-fed lakes is largely determined by the heavy sediment input of inflowing rivers during the glacier-melting period in summer. Sedimentary processes common to these lakes are prograding delta sedimentation, resedimentation by debris flows and turbidity currents from slumping on the delta front, suspension fallout from river-induced overflows and interflows, and sedimentation by river-induced underflows (or river-induced turbidity currents) (e.g., Gilbert, 1975; Sturm and Matter, 1978; Smith et al., 1980; Smith and Ashley, 1985; Weirich, 1986; Chikita et al., 1991). In this study, sediment-laden underflows, induced by the heavy sediment input of a river, are referred to

bottom currents flowing continuously on an undulated bottom bed of lake, with keeping suspended sediment concentration higher than the upper water. They were observed along the elongated and undulated bottom bed of glacier-fed Peyto Lake, Canada during the glacier-melting period (Smith et al., 1980; Chikita et al., 1991). By measuring lake currents and light transmissivity, and trapping suspended sediment, Smith et al. (1980) showed that the sediment-laden underflows exercise a great effect on sedimentation over the Peyto Lake basin. Chikita et al. (1991) examined the physical mechanism of sedimentation by the underflows. As a result, by noting a difference in the driving force, they classified the sediment-laden underflows into "turbidity currents" and "bottom suspension flows". The former are driven by the downslope component of the gravity force, while the latter flowing upslope are probably generated as part of locally strong wind-driven currents due to a downlake katabatic wind.

In this study, sediment sorting processes of the sediment-laden underflows based on their dynamic behavior are described using the spatial distributions of sedimentation rate and statistical grain size parameters for the sediment trapped for June–August of 1987, and the sedimentary facies of trapped-sediment columns are related to a variation in the river sediment input resulting from a specific change in weather conditions.

2. Study area and methods

The field survey in Peyto Lake, Alberta, Canada (51°43.5'N, 116°31'W) was performed during the glacier-melting period (June–August) of 1987 (Fig. 1; see also Chikita et al., 1991). A braided inflowing river, Peyto Creek supplies the lake water dominantly from Peyto Glacier in this season. The water discharge, water temperature and suspended sediment concentration of the river were observed by a stage recorder, a thermistor thermometer and frequent water sampling, respectively at the upstream head of a braided outwash plain (Chikita et al., 1991). The sediment concentration and water temperature of inflowing water were measured also at the mouth of the greatest distributary which was 80 m distant from A. Meanwhile, at A, B and C, the sediment-laden underflows were observed by vertically measuring lake currents, water temperature and sediment concentration. The downstream end of the outwash plain (i.e., the delta front) is connected by the subaqueous foreset slope of about 11° averaged over 0–30 m depth. The sediment discharge of Peyto Creek formed several surface sediment plumes at most 100 m long off the delta front. Peyto Lake lies along the bottom of a U-shaped valley, giving the morphometry of the elongated

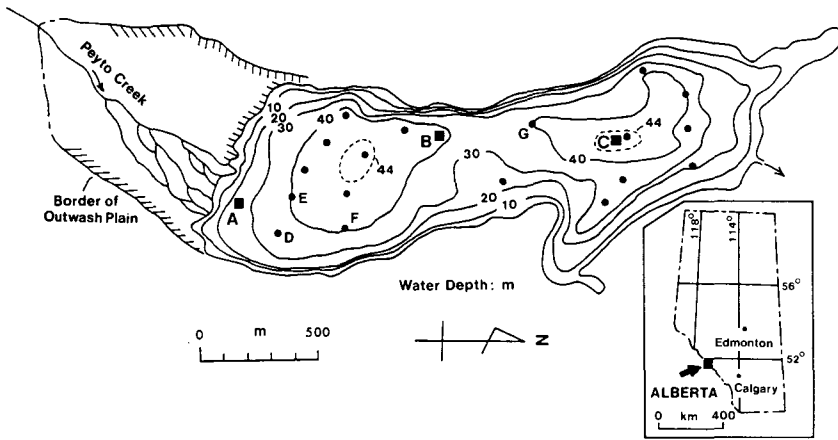


Fig. 1. Bathymetric map of Peyto Lake (after Smith et al., 1980), and locations of three stations (A, B and C) observing lake currents and 18 stations (solid circles) trapping sediment near the bottom. Deposits trapped at D, E, F and G were vertically analyzed on grain size. The two deepest regions are shown by dashed isobaths (44 m depth) measured in August 1987.

lake basin which is divided into two subbasins by a middle subaqueous sill. The lake has a drainage area of 45 km², including a water surface area of 1.4 km² and a glacier-covered (Peyto Glacier) area of 13 km². The geology of the drainage basin is Precambrian and Cambrian argillite, limestone and dolomite.

Sediment traps were set at 18 stations (solid circles in Fig. 1) at 0.3 m above the bottom. They were fixed underwater with a moored buoy-sandbag system for 41–44 days from 29 June 1987. Referring to the review of Blomqvist and Hankanson (1981), the cylindrical traps of $H/D > 3$ (height, $H = 0.31$ m; diameter, $D = 0.055$ m) were used. Just after the recovery of the traps, the thickness of deposits was measured, and their sedimentary facies were examined. The porosity of the deposits was determined in a laboratory by drying at 110°C more than 5 hrs.

Grain size analysis was performed for the total deposits trapped at each station by a photo-extinction (settling) method with a centrifuge for $d < 44 \mu\text{m}$, and sieving for $d > 44 \mu\text{m}$. The sediment trapped at D, E, F and G was also vertically analyzed by subsampling the sediment columns (Fig. 1). During the grain size analysis, no flocculation occurred in suspension of the sediment concentration 200–300 mg/l, even if not using a dispersant. As mentioned below, this is probably because the sediment settling in distilled water mostly consists of incohesive dolomitic grains. The sediment-laden underflows obser-

ved in Peyto Lake exhibited electric conductivity of 127–133 $\mu\text{S}/\text{cm}$ (thus almost no salinity expected) and suspended sediment concentration of 20–80 mg/l (Smith et al., 1980; Chikita et al., 1991). The suspended sediment in the underflows thus seems to have behaved as “cohesionless” or “completely discrete”. Using an X-ray diffractometer, the mineralogy of the trapped sediment was examined for sand- and silt-sized grains of 31–250 μm and clay-sized grains smaller than 2 μm . The former were pulverized to the order of 1 μm with a crusher before the analysis.

The life span of Peyto Lake was estimated using the aerial photography and horizontal distributions of sedimentation rate based on the sediment trapping.

3. Dynamic behavior of sediment-laden underflows

Figure 2 shows vector diagrams of horizontal lake currents at each depth and vertical profiles of water temperature and suspended sediment concentration, obtained at A, B and C (see also Chikita et al., 1991). For 14–15 July 1987 when the observations were performed, inflowing water at the mouth of the greatest distributary indicated sediment concentration of 570–1,080 mg/l and water temperature of 4–6°C. The bulk density, 1000.37–1000.67 kg/m^3 of the inflowing suspension, calculated from the above is always greater than that of the lake water, 999.73–1000.00 kg/m^3 at sediment concentration of $< \sim 5 \text{ mg}/\text{l}$ and temperature of 6–10°C. Meanwhile, the inflowing suspended sediment consisted of silt and clay more than 70–90 wt.% (Chikita et al., 1991). The inflowing suspension thus plunged within 70 m offshore after forming the surface sediment plumes released from the mouths of several distributaries. Station A was 10 m off the plunging point of the greatest sediment plume. As a result, the turbid water was found at a depth of more than 10 m at A. The northward flow direction corresponds to a direction of the maximum slope angle on the downslope bed at A. The bottom flow at A thus proves to be river-induced turbidity currents driven by gravity. The turbid flow at more than 30 m depth of B is regarded as “bottom suspension flows” driven by wind-driven currents (Chikita et al., 1991). The term “sediment-laden underflows” is used to comprise two dynamically different bottom flows, turbidity currents and bottom suspension flows. Concerning the bottom suspension flows at B, the measurements of light transmissivity by Smith et al. (1980) revealed that against the downslope component of the gravity force, the turbid bottom water could flow up the sill slope north of B. As a result, the sediment-laden underflows may get over the sill and then go down to a northmost region near an outlet (see Fig. 6 in Chikita et al.,

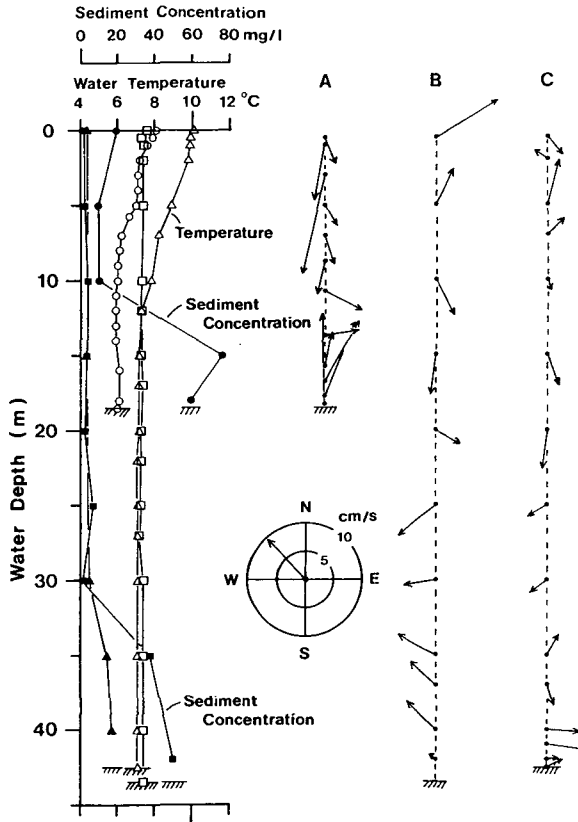


Fig. 2. Vertical profiles of water temperature and suspended sediment concentration at A (circles), B (squares) and C (triangles), and horizontal flow velocity averaged for 50 sec at each depth of the three stations (revised from Chikita et al., 1991).

1991). To go up the sill slope the sediment-laden underflows should get the great inertial force at the origin near A or receive the new supply of kinetic energy between A and B, because the underflows produced near the river-mouths (i.e., river-induced turbidity currents observed at A) first go down the foreset slope of the delta, but lose the driving force at a maximum-depth region between A and B (see Fig. 1). Exceptionally strong wind-driven currents at a depth of more than 30 m at B (Fig. 2), however, show that around B, the bottom water could get the new turbulent energy enough to prevent the sediment deposition. The deep strong wind-driven currents held the northward component in motion. The sediment-laden underflows driven by wind-driven currents (here the bottom suspension flow) are thus allowed to pass over the middle sill

as part of the wind-driven currents. The eastward turbid flow near the bottom at C is considered as weak turbidity currents which are driven by gravity, but are dynamically influenced by lake currents induced by the river-outflow (Chikita et al., 1991).

4. Mineralogy and grain size of sediment

Table 1 shows the mineralogy of sand- and silt-sized grains (31–250 μm) and clay-sized grains ($<2\ \mu\text{m}$) for the total sediment trapped in the summer of 1987. As a result, it includes a great amount of such calcareous minerals as dolomite and calcite, and negligibly a cohesive clay mineral (i.e., amesite belonging to kaolinite-serpentine group of 1:1 type; see Bailey, 1980). It should be noted that the so-called “clay minerals” occupy only part of the mineralogy of “clay-sized grains”. The mineralogy of the sediment is not thus dominated by such cohesive clay minerals as montmorillonite, chlorite, etc. This is probably because most of the fine sediment was yielded from the bedrock (mainly dolomite) erosion by the mass movement of Peyto Glacier and then washed out quickly from inside Peyto Glacier: The fine sediment was not thus exposed to the chemical weathering for a long period. The trapped sediment included only a little organic matter as shown by 0.75–1.6% of ignition loss (Fig. 11 in Chikita et al., 1991). The electric conductivity of the sediment-laden underflows measured by Smith et al. (1980) ranged over 127–133 $\mu\text{S}/\text{cm}$, thus showing almost non-salinity. These results suggest that the “discreteness” of the sediment judged in the grain size analysis is applicable as its original behavior in suspension of the sediment-laden underflows. The observational results of Smith et al. (1980) and Chikita et al. (1991) show that the underflows dominate the offshore sedimentation in Peyto Lake. The grain size distributions of the trapped sediment thus present directly the characteristics of the sediment sorting processes of the underflows controlled by their dynamic behaviors.

Table 1. Main minerals (for 31–250 μm and $<2\ \mu\text{m}$ grains) contained in trapped deposits. Numerical values in parentheses show the relative peak intensity among the minerals identified with an X-ray diffractometer.

Minerals (31–250 μm)		Dolomite		Calcite		Quartz	
Lattice Spacing, Å		2.90 (10)		3.04 (1)		3.35 (1)	
Minerals ($<2\ \mu\text{m}$)	Dolomite	Aragonite	Muscovite	Calcite	Amesite	Quartz	
Lattice Spacing, Å	2.88 (10)	3.40 (10)	9.94 (6)	3.03 (3)	7.05 (2)	3.34 (2)	

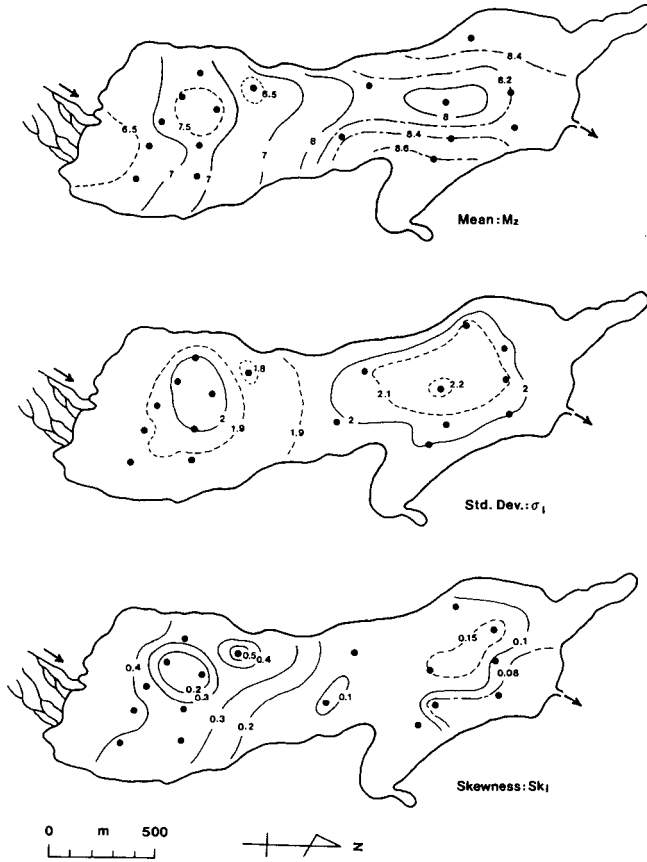


Fig. 3. Horizontal distributions of mean M_z , standard deviation σ_1 and skewness Sk_1 for deposits trapped for 41-44 days from 29 June 1987 (see text for more detail).

Figure 3 shows spatial distributions of mean M_z , standard deviation σ_1 and skewness Sk_1 on grain size for the total deposits trapped over the period 29 June to 9-12 August 1987. The three grain size parameters expressed in phi scale ($\phi = -\log_2 (10^{-3} \times d)$; d , grain diameter in μm) were calculated by a graphic method, using the following equations (Folk and Ward, 1957).

$$M_z = (\phi_{16} + M_{d\phi} + \phi_{84})/3 \quad (1)$$

$$\sigma_1 = (\phi_{84} - \phi_{16})/4 + (\phi_{95} - \phi_5)/6.6 \quad (2)$$

$$Sk_1 = \{\alpha_\phi + (\phi_5 + \phi_{95} - 2M_{d\phi})/(\phi_{95} - \phi_5)\}/2 \quad (3)$$

where ϕ_5 , ϕ_{16} , $M_{d\phi}$, ϕ_{84} and ϕ_{95} are phi values of 5, 16, 50, 84 and 95 percentiles, respectively on a grain size cumulative curve. $\alpha_\phi = (M_\phi - M_{d\phi}) / \sigma_\phi$, $\sigma_\phi = (\phi_{84} - \phi_{16}) / 2$ and $M_\phi = (\phi_{16} + \phi_{84}) / 2$ are skewness, standard deviation and mean, respectively, proposed by Inman (1952). According to the Wentworth-Lane scale (e.g., see Fig. 3-6 in Pettijohn, 1975), the trapped sediment was, as a whole, composed of fine sand ($250 > d > 125 \mu\text{m}$ or $3 > \phi > 2$), very fine sand ($125 > d > 62.5 \mu\text{m}$ or $4 > \phi > 3$), silt ($62.5 > d > 3.9 \mu\text{m}$ or $8 > \phi > 4$) and clay ($d < 3.9 \mu\text{m}$ or $\phi > 8$). It should be noted that increases of M_z and σ_1 present decreasing mean grain size and relatively poor sorting, respectively, and an increase in positive Sk_1 shows an increase in the relative amount of grains belonging to the relatively large size region in a size frequency distribution. Sediment sorting by the sediment-laden underflows is thus characterized as follows:

(1) The turbidity currents, originated from near the mouths of inflowing distributaries, deposited relatively coarse grains from the bottom suspension, with decreasing mean size and skewness and increasing standard deviation toward the proximal deepest region. This shows that the size frequency distribution of deposits approaches the symmetrical one toward the deepest region, due to the fast deposition of relatively large grains, but the gradual increase in deposition of relatively small grains then causes the poor sorting. Since the driving force (i.e., the downslope component of gravity force) of the turbidity currents is lost in the deepest region, the consequent, relatively great deposition of silt and clay raised the maximum of M_z and σ_1 , and the minimum Sk_1 .

(2) North of the proximal deepest region, there appear the minimums of M_z and σ_1 and the maximum of Sk_1 . This presents the new supply of kinetic energy to the bottom suspension, probably by the locally strong wind-driven currents: The silt- and clay-sized grains transported by the turbidity currents thus keep suspended because of their slow settling (the order of 10^{-5} m/s), and move farther with following the dynamic behaviors of wind-driven currents. The consequently formed "bottom suspension flows" pass over the middle sill, followed by the weak turbidity currents flowing down the northern slope. Their sediment sorting is represented by increasing M_z and σ_1 , and decreasing Sk_1 toward the distal deepest region, which is similar to that by the proximal turbidity currents.

(3) The open region of $M_z < 8.2$, $\sigma_1 > 2$ and $Sk_1 > 0.1$ in the northern sub-basin, however, shows that the sediment sorting by the distal turbidity currents is already declined. At C in the northern deepest region, sediment-laden underflows moved eastwards (Fig. 2). This suggests that dynamics of the

bottom suspension at C is influenced by lake currents which are induced by the river outflow, and thus flow toward a river outlet. In a northmost region ranging from the northern deepest region to the river outlet, the mean size and σ_1 decrease slightly, and Sk_1 approaches zero (i.e., a symmetrical size frequency). This is probably because sediment sorting is performed by the lake currents due to the outflow, and meanwhile very fine suspended sediment, selectively discharged from the outlet, increases in quantity, as the bottom suspension approaches

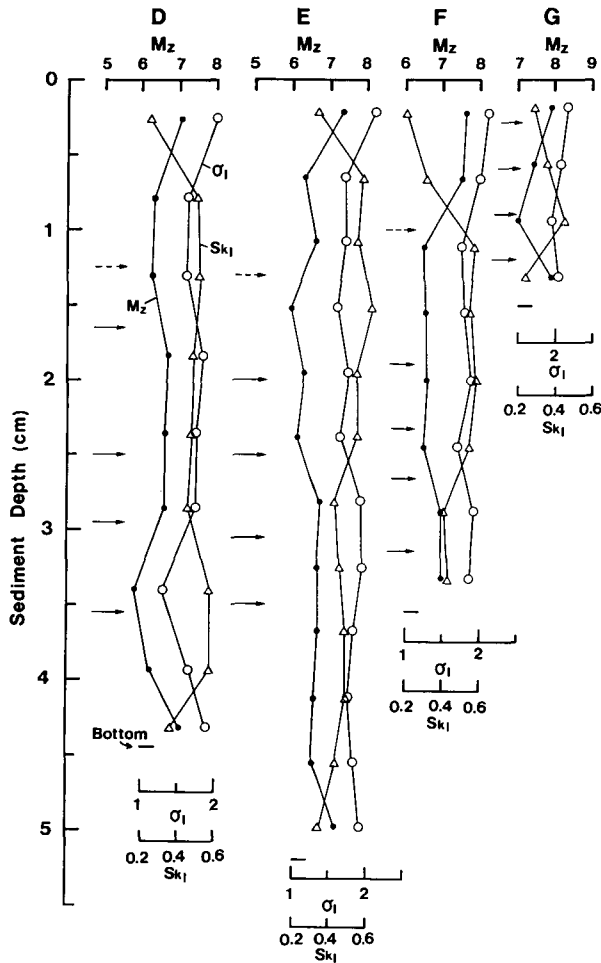


Fig. 4. Vertical profiles of the three grain size parameters, M_z , σ_1 and Sk_1 for deposits trapped at D, E, F and G. Solid and dotted arrows show locations of clear and unclean organic-rich layers, respectively.

the outlet.

Corresponding to the grain size of trapped sediment, the bottom and suspended sediments obtained at A, B and C were mostly composed of fine grains less than $250\ \mu\text{m}$ (see Fig. 10 in Chikita et al., 1991). Their depositional or erosional condition under the shear force of the sediment-laden underflows were examined by applying the drag law and using the new "extended Shields diagram" proposed by Chikita (1990) (Chikita et al., 1991).

Figure 4 shows vertical profiles of the three grain size parameters, M_z , σ_1 and Sk_1 for deposits trapped at D, E, F and G (Fig. 1). Just after the recovery of sediment traps, the accumulated deposits were 5.1 cm, 6.2 cm, 4.5 cm and 2.3 cm thick at D, E, F and G, respectively, but became finally 4.45 cm, 5.2 cm, 3.55 cm and 1.5 cm thick, respectively, due to the natural compaction. The grain size analysis was performed by subsampling the compacted deposits by 0.38–0.53 cm in thickness. As a vertical tendency common to the four deposits, it is seen that as the grain size decreases (i.e., M_z increases), the standard deviation increases and the skewness decreases. This result corresponds to the horizontal tendency in the sediment sorting by turbidity currents (Fig. 3). This means that the four trapped sediments were deposited under sorting by turbidity currents of an unsteady state caused by a temporal variation in sediment discharge of Peyto Creek. Four or five organic-rich black layers of 1–3 mm in thickness were seen in columns of trapped deposits (arrows in Fig. 4). They

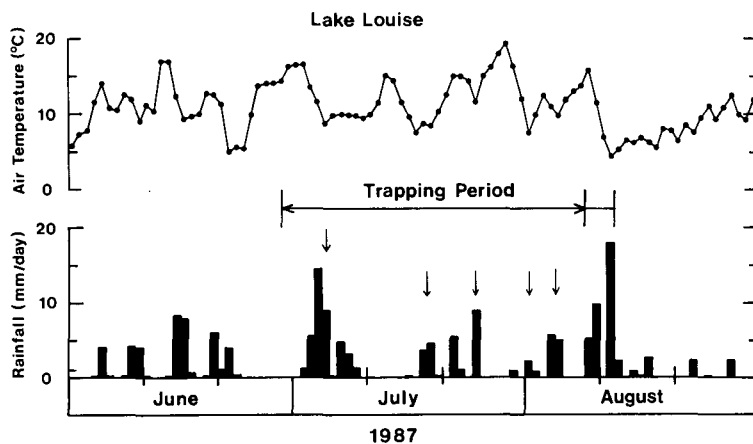


Fig. 5. Daily air temperature and rainfall recorded at the weather station of Lake Louise for June–August 1987. All the sediment traps were recovered over 9–12 August 1987. Cold rainfalls occurred five times (arrows) for the sediment-trapping period.

were found for 12 traps, and occupied in space 9.8% of the 18 trapped deposits. As pointed out by Chikita et al. (1991), they were probably formed from the surface discharge eroding organic-rich soils on steep slopes around the lake. The surface discharge is raised by summer rainfalls always occurring under cold weather condition. The glacier-melting discharge is then relatively suppressed, and instead the rainfall discharge dominates the organic-sediment supply. Meteorological records at the weather station of Lake Louise, 40 km south-southeast of Peyto Lake indicate that during the trapping period 29 June to 9–12 August 1987, such cold rainfalls occurred five times (Fig. 5). This number accords to that of the organic-rich layers in the sediment columns of D, E and F. An unclear organic-rich layer existed at D, E and F (dotted arrows in Fig. 4), but the G deposits did not hold it. This is possibly because the rainfall of 4–5 August (i.e., the last rainfall during the trapping period; Fig. 5) occurred under relatively warm condition, thus exalting the glacier-melting. The organic-rich layers, found from off the delta front to G (Fig. 1), decreased their thickness offshore, but did not change it transversely. This suggests that the suspension from the surface discharge flowed into the lake in terms of a uniform sheet flow on the outwash plain, and then dispersed in the form of overflows or interflows.

5. Sedimentation rate and life span

The life span of Peyto Lake was estimated by using the data of offshore sedimentation rate given by Smith et al. (1980) and Chikita et al. (1991), and the aerial photography for delta progradation.

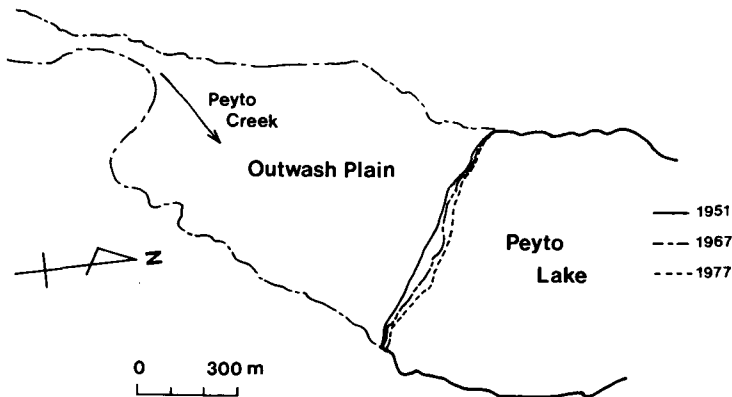


Fig. 6. Variations in the topography of delta front, based on three aerial photographs taken in the summers of 1951, 1967 and 1977.

Figure 6 shows a topographic change of the delta front obtained by three aerial photographs taken in the summers of 1951, 1967 and 1977. This was obtained by best fitting lateral borderlines of the outwash plain bounded by the U-shaped valley. The mean offward speed of delta front obtained from Fig. 7 is 1.46 m/yr averaged for 1951-1967 and 1.41 m/yr for 1967-1977. Assuming that the foreset-slope angle at 0-20 m depth in Fig. 1 is consistently constant ($=21^\circ$), sedimentation rate by delta progradation is estimated at 2.07×10^4 - 2.14×10^4 m³/yr or 2.92×10^4 - 3.02×10^4 metric tons per year using the porosity, 0.5 and the grain density, 2.823 g/cm³. An estimate of annual offshore sedimentation rate is made on the base of the sediment trapping in summer by Smith et al. (1980) and Chikita et al. (1991), because water discharge of Peyto Creek for June-September accounts for 90% of the total annual inflow (Derikx, 1972), and thus all the sediment input is possibly concentrated in this season. Mean mass sedimentation rate in traps, averaged over the lake basin, was 0.0446 g/cm²/day for 19 June-1 September 1976 (Smith et al., 1980) and 0.0611 g/cm²/day for 41-44 days from 29 June 1987 (Chikita et al., 1991). Hence sedimentation rate is given 0.0434 cm/day and 0.0595 cm/day, respectively, using the mean porosity, 0.64 and the grain density, 2.823 g/cm³. The total amount of offshore sedimentation is thus estimated at 4.56×10^4 m³ or 4.68×10^4 metric tons for the 75-day period of 1976 (Smith et al., 1980) and at 3.58×10^4 m³ or 3.68×10^4 metric tons for the 41-44 days in 1987. Considering a difference of the trapping period, these results accord reasonably in spite of different hydrology of Peyto Creek during the trapping period. Offshore sedimentation is determined largely by the sediment-laden underflows and slightly by sediment fallout through the overflows or interflows caused by the surface discharge. The latter occupies 9.8% of the offshore sedimentation. I here assumed that the above sedimentation amount by Smith et al. (1980) presents the annual sediment input to a offshore region, with keeping constant for 1951-1977, and the overflows' and/or interflows' contribution (9.8%) to the offshore sedimentation does not change consistently. The life span of Peyto Lake is then estimated at 586 yrs, and the delta progradation, the sediment-laden underflows and the overflows and/or interflows provide 32%, 61% and 7%, respectively of the total sedimentation.

6. Conclusions

The measurements of water temperature, suspended sediment concentration and flow velocity, conducted in Peyto Lake during the glacier-melting period of 1987, revealed that the bottom suspension flows in the form of two

dynamically different underflows, i. e., "turbidity currents" driven by gravity and "bottom suspension flows", probably driven by wind-driven currents. Sediment sorting processes of the sediment-laden underflows are consistently explained by horizontal distributions of mean, standard deviation and skewness on grain size for trapped deposits. Annual sedimentation rates at delta front and in an offshore region were estimated by using aerial photographs and horizontal distributions of the trapped-deposit amount, respectively. As a result, the delta progradation, the sediment-laden underflows and overflows and/or interflows account for 32%, 61% and 7%, respectively of the total lake sedimentation, and the possible life span of Peyto Lake was given at 586 yrs.

Acknowledgments

I would like to express special thanks to Dr. L. Cammaert, Associate Vice-President, the University of Calgary, Canada for her generous assistance and advice. I also thank Mr. N. Yonemitsu, the University of Alberta, Canada, Mr. M. Yoshida, Hokkaido University and Mrs. Y. Chikita for their great assistance in the field survey, and Dr. J. Ishii, Tokai University and Ms. K. Freeman, the University of Calgary, Canada for their welcome support in the sample analyses. This study was partially supported by the Universities Coordinating Council, the Government of Alberta, Canada. Dr. R. Gilbert, Queen's University, Canada and Dr. N.D. Smith, the University of Illinois, U.S.A. gave constructive criticisms to the first version of this manuscript.

References

- Bailey, S.W., 1980. Structures of layer silicates. Crystal structures of clay minerals and other X-ray identification (ed. G.W. Brindley and G. Brown). Mineralogical Society Monograph, No. 5, Mineralogical Society, London, 1-124.
- Blomqvist, S. and L. Hankanson, 1981. A review on sediment traps in aquatic environments. *Archiv für Hydrobiologie*, **91**, 101-132.
- Chikita, K., 1990. Sedimentation by river-induced turbidity currents: Field measurements and interpretation. *Sedimentology*, **37**, 891-905.
- Chikita, K., N. Yonemitsu and M. Yoshida, 1991. Dynamic sedimentation processes in a glacier-fed lake, Peyto Lake, Alberta, Canada. *Jpn. J. Limnol.*, **52**, 27-43.
- Derikx, L., 1972. Hydrological characteristics of Peyto Glacier. Guidebook to the Intern. Symp. on the Role of Snow and Ice in Hydrology, Banff, Alberta, Can. Nat. Comm. for the Intern. Hydrol. Decade, 79-84.
- Folk, R.L. and W.C. Ward, 1957. Brazos River bar: A study in the significance of grain size parameters. *J. Sediment. Petrol.*, **27**, 3-26.
- Gilbert, R., 1975. Sedimentation in Lillooet Lake, British Columbia. *Can. J. Earth Sci.*, **12**, 1697-1711.

- Inman, D.L., 1952. Measures for describing the size distribution of sediments. *J. Sediment. Petrol.*, **22**, 125-145.
- Pettijohn, F.J., 1975. *Sedimentary rocks*. Harper & Row, Publishers, New York, 628 pp.
- Smith, N.D. and G. Ashley, 1985. Proglacial lacustrine environment. *Glacial Sedimentary Environments* (ed. G.M. Ashley, J. Shaw and N.D. Smith), Soc. Paleontol. Mineral., Short Course, No. 16, Chapter 4, 135-215.
- Smith, N.D., M.A. Venol and S.K. Kennedy, 1980. Comparison of sedimentation regimes in four glacier-fed lakes of Western Alberta. *Proc. 6th Guelph Symp. on Geomorph.*, the Univ. of Guelph, Guelph, 203-238.
- Sturm, M. and A. Matter, 1978. Turbidites and varves in Lake Brienz (Switzerland) : Deposition of clastic detritus by density currents. *Spec. Publ., Intern. Assoc. Sediment.*, **2**, 147-168.
- Weirich, F., 1986. The record of density-induced underflows in a glacial lake. *Sedimentology*, **33**, 261-277.